Neuroendocrine regulatory peptide-2 stimulates glucose-induced insulin secretion *in vivo* and *in vitro*

Abu Saleh Md. Moin [a,1], Hideki Yamaguchi [a,1], Marie Rhee [b], Ji-Wom Kim [b], Koji Toshinai [a], T.M. Zaved Waise [a], Farhana Naznin [a], Takashi Matsuo [a], Kazuki Sasaki [c], Naoto Minamino [c], Kun-Ho Yoon [b], Masamitsu Nakazato [a,*]

[a] *Division of Neurology, Respirology, Endocrinology and Metabolism, Department of Internal Medicine, Faculty of Medicine, University of Miyazaki, 5200 Kihara, Kiyotake, Miyazaki 889-1692, Japan*
[b] *Department of Endocrinology and Metabolism, The Catholic University of Korea, 505 Banpodong, Seochogu, Seoul 137-040, Republic of Korea*
[c] *Department of Molecular Pharmacology, National Cerebral and Cardiovascular Center Research Institute, 5-7-1 Fujishirodai, Suita, Osaka 565-8565, Japan*

ARTICLE INFO

ABSTRACT

Neuroendocrine regulatory peptide (NERP)-2, recently identified as a bioactive peptide involved in vasopressin secretion and feeding regulation in the central nervous system, is abundantly expressed in endocrine cells in peripheral tissues. To explore the physiological roles of NERP-2 in the pancreas, we examined its effects on insulin secretion. NERP-2 increased glucose-stimulated insulin secretion (GSIS) in a dose-dependent manner, with a lowest effective dose of 10^{-7} M, from the pancreatic β-cell line MIN6 and isolated mouse pancreatic islets. NERP-2 did not affect insulin secretion under the low-glucose conditions. Neither NERP-1 nor NERP-2–Gly (nonamidated NERP-2) stimulated insulin secretion. NERP-2 significantly augmented GSIS after intravenous administration to anesthetized rats or intraperitoneal injection to conscious mice. We detected NERP-2 in pancreatic islets, where it co-localized extensively with insulin. Calcium-imaging analysis demonstrated that NERP-2 increased the calcium influx in MIN6 cells. These findings reveal that NERP-2 regulates GSIS by elevating intracellular calcium concentrations.

1. Introduction

VGF is a 617-amino acid neurosecretory protein originally identified as a product of the nerve growth factor-responsive gene *Vgf* in rat pheochromocytoma PC12 cells [1,2]. The *Vgf* gene is expressed in subsets of neurons and specific populations of endocrine cells [3–5]. VGF has several paired basic amino acid residues that represent potential cleavage sites for the tissue-specific prohormone convertases PC1/3 and PC2. Several lines of evidence suggest that VGF is a precursor of multiple bioactive peptides with a variety of biological functions [6–9]. We identified two novel biologically active peptides, neuroendocrine regulatory peptides (NERP)-1 and NERP-2, by comprehensive analysis of C-terminally amidated peptides secreted by a thyroid medullary carcinoma cell line [10]. Human NERP-1 is a 26-amino acid peptide derived from

VGF amino acids 281–306, and human NERP-2 is a 38-amino acid peptide derived from a distinct portion of VGF, amino acids 310–347. In the hypothalamus of rats and humans, NERPs co-localize with the antidiuretic hormone vasopressin in the storage granules of the paraventricular and supraoptic nuclei [10]. Administration of NERPs suppresses vasopressin release from the hypothalamus and pituitary, both *in vitro* and *in vivo*. NERP-2 is also abundant in the lateral hypothalamic area, an orexigenic center, where it functions in the control of food intake and energy homeostasis via the orexin pathway [11]. The C-terminal amidation of NERPs is required for these biological activities.

To investigate the biological functions of NERPs in the pancreas, we studied their expression and localization in the pancreas of rodents, and monitored their effects on insulin secretion in the pancreatic β-cell line MIN6 and isolated mouse pancreatic islets. NERP-2, but not NERP-1, enhanced glucose-stimulated insulin secretion (GSIS). We also examined the effects of peripheral administration of NERP-2 on insulin secretion in rats and mice. Finally, we performed calcium-imaging analysis to study the effect of NERP-2 on intracellular calcium influx in MIN6 cells. Our results suggest that NERP-2 serves as an insulinotropic peptide in β-cells.

2. Materials and methods

2.1. Animals

C57BL/6 J mice (9-week-old male, Charles River Laboratories, Yokohama, Japan), *Vgf* knockout mice on B6 background (9-week-old male, provided by Dr. Stephen R. J. Salton, Mount Sinai School of Medicine, NY) [12], and Wistar rats (9-week-old male, Charles River Laboratories) were maintained in individual cages under controlled temperature (21–23 °C) and light (light on: 08:00–20:00) conditions with *ad libitum* access to food and water. All animal experiments were performed in accordance with the Japanese Physiological Society's guidelines for animal care.

2.2. Immunohistochemistry

For 3,3′-diaminobenzidine (DAB)-based immunostaining, the pancreata of C57BL6/J and *Vgf* knockout mice were immersed in 4% paraformaldehyde for 24 h at 4 °C, incubated for 24 h in PBS containing 30% sucrose, quickly frozen on dry ice, and cut into 7-μm slices with a cryostat at −20 °C. After treatment with 1% normal goat serum, serial sections were incubated overnight at 4 °C with rabbit anti-NERP-1 antiserum (final dilution 1:1000) or rabbit anti-NERP-2 antiserum (final dilution 1:2000). Antibodies specific for NERP-1 or NERP-2 were prepared as described elsewhere [10]. The samples were then incubated with biotinylated goat anti-rabbit IgG at room temperature for 2 h. The signals were amplified using the ABC Kit (Vector Laboratories, Inc., Burlingame, CA), and visualized using the Peroxidase Substrate Kit (Vector Laboratories, Inc.) on a Nikon A1si microscope (Nikon, Tokyo, Japan).

For double immunofluorescence staining, C57BL6/J mouse pancreata were prepared as described above. Slices were incubated with 1% normal donkey serum for 60 min at room temperature. After overnight incubation at 4 °C with guinea-pig anti-insulin antiserum (DAKO, Carpinteria, CA), slices were washed with PBS and then incubated with Alexa FluorTM 488 donkey anti-guinea-pig IgG (Molecular Probes, Inc., Eugene, OR) at room temperature for 2 h. After blocking in normal goat serum, samples were incubated overnight at 4 °C with rabbit anti-NERP-2 antiserum (final dilution 1:2000). Finally, samples were incubated with Alexa FluorTM 568 goat anti-rabbit IgG (Molecular Probes) for 2 h at room temperature and incubated with DAPI (4,6-diamidine-2-phenylindole dihydrochloride, Roche, Mannheim, Germany, dilution 1:10,000) for 10 min. They were imaged using an OLYMPUS AX-7 fluorescence microscope (Olympus, Tokyo, Japan).

2.3. In vitro study

The insulinoma cell line MIN6 (provided by Dr. K. Minami, University of Chiba, Japan) was cultured in Dulbecco's modified Eagle's medium (DMEM) containing 25 mM glucose with 4 mM L-glutamine and 10% heat-inactivated fetal bovine serum (FBS) (Nichirei Biosciences Inc., Tokyo, Japan) in sterile plastic plates (100 mm, Asahi Techno Glass, Chiba, Japan) for 5 days. When the cells reached 60–80% confluence, they were plated (10^5 cells/well) in 48-well plates (10 mm, Asahi Techno Glass) and cultured for 48 h. Cells were washed with HEPES-balanced Krebs-Ringer bicarbonate (HKRB) buffer (119 mM NaCl, 4.74 mM KCl, 2.54 mM $CaCl_2$, 1.19 mM $MgCl_2$, 1.19 mM KH_2PO_4, 25 mM $NaHCO_3$, 10 mM HEPES, 0.2% bovine serum albumin (BSA), pH 7.4) and pre-incubated for 30 min in HKRB containing 1 mM glucose; they were then incubated for 1 h in HKRB buffer containing 5.5 mM or 22 mM glucose with or without rat NERP-1 (10^{-6} M), NERP-2 (10^{-6} M), NERP-2-Gly (10^{-6} M) (Peptide Institute, Osaka, Japan) or human GLP-1 (10^{-8} M) (CS Bio Co., Menlo Park, CA). Insulin secreted into the medium was measured using the Mouse Insulin EIA Kit (Morinaga Institute of Biological Science, Inc., Yokohama, Japan).

Pancreatic islets were isolated (50–80 islets per mouse) from 9-week-old male C57BL/6 J mice anesthetized with pentobarbital (60 mg/kg body weight (BW), intraperitoneal (i.p.)) (Dainippon Sumitomo Pharma, Osaka, Japan) by a modified collagenase digestion method [13]. Ice-cold collagenase (Roche Applied Science, Mannheim, Germany) solution was injected into the common bile duct at a concentration of 1 mg/ml in Hanks balanced salt solution (HBSS) (Invitrogen, Grand Island, NY). The distended pancreas was removed, placed in ice-cold collagenase solution (1 mg/ml), and minced with scissors. The mixture was placed in a 37 °C water bath for 15 min with shaking. Digestion was stopped by the addition of ice-cold HBSS, and samples were then centrifuged (200g) for 1 min at 4 °C. The pellet was resuspended in HBSS. Centrifugation and resuspension were repeated several times to remove the exocrine tissues. Islets were hand-picked under a stereomicroscope (Nikon, Tokyo, Japan). Groups of ten individual islets were placed in single polystyrene tubes and cultured in RPMI 1640 medium (Nacalai Tesque, Inc., Kyoto, Japan) supplemented with 10% heat-inactivated FBS, 10,000 U/ml penicillin G, 10 mg/ml streptomycin, and 25 μg/ml amphotericin B with 11 mM glucose in a humidified 95% air/5% CO_2 atmosphere at 37 °C for 24 h. The islets were washed with HKRB buffer, pre-incubated in low glucose (2.8 mM) solution at 37 °C for 30 min, and then incubated with high glucose (16.7 mM) containing rat NERP-1 (10^{-6} M), NERP-2 (10^{-6} M, 10^{-7} M, or 10^{-8} M), NERP-2-Gly (10^{-6} M), or human GLP-1 (10^{-8} M) for 1 h. Insulin secreted into the medium was measured using the Mouse Insulin EIA Kit. MIN6 cells or islets were lysed in Radio-Immunoprecipitation Assay buffer (Nacalai Tesque, Inc.) and total protein was determined using Protein Assay Kit I (Bio-Rad, Hercules, CA).

2.4. In vivo study

C57BL/6 J mice (9-week-old male, $n = 6$–8 for each group) were fasted for 18 h, and then injected i.p. with glucose (1 g/kg BW) with or without rat NERP-2 (500 nmol/kg BW) or human GLP-1 (4 nmol/kg BW). Blood was collected by tail-prick at time points ranging from 10 min before peptide administration to 90 min after peptide administration. Plasma insulin was determined using the Mouse Insulin EIA Kit.

Wistar rats (9-week-old male, $n = 6$–8 for each group) fasted for 18 h were anesthetized with pentobarbital (50 mg/kg BW), and a catheter was placed in each animal's right femoral vein. Rats were injected intravenously (i.v.) with 400 μl glucose (500 mg/kg BW) or 400 μl glucose containing rat NERP-2 (30 nmol/kg BW) or human GLP-1 (10 pmol/kg BW). Blood was collected by tail-prick at time points ranging from 10 min before peptide administration to 40 min after peptide administration. Plasma insulin was determined using the Rat Insulin EIA Kit (Morinaga Institute of Biological Science, Inc.).

2.5. Measurement of intracellular Ca^{2+} influx ($[Ca^{2+}]_i$)

Ca^{2+} imaging was performed under continuous perfusion of MIN6 cells with HKRB buffer at a flow rate of 200 μl/min at 37 °C. Cells were imaged using a cooled charge-coupled device camera, and the ratio image was generated in the Functional Imaging Cell-Sorting System (IMACS; Hamamatsu Photonics, Hamamatsu, Japan). Images were captured at 15-s intervals; 340- and 380-nm excitation filters and a 510-nm emission filter were used for Fura-2 dual-wavelength excitation-ratio imaging [14]. Changes of $[Ca^{2+}]_i$ were calculated from changes in the 340-to-380 fluorescence ratio. MIN6 cells were loaded with

1 μM Fura-2 acetoxymethyl ester (Dojindo, Kumamoto, Japan) in HKRB at 37 °C for 20 min. After 10-min perfusion with 2.8 mM glucose in HKRB, the medium was changed to HKRB containing 2.8 mM glucose, 22 mM glucose, 22 mM glucose with 1 μM NERP-2, 22 mM glucose with 1 μM NERP-2-Gly, or 22 mM glucose with 10 nM GLP-1, and the ratio was recorded for 20 min. At the end of each experiment, MIN6 cells were exposed to 100 nM tolbutamide (Sigma–Aldrich, St. Louis, MO) for 5 min. All data were expressed as percent changes from the average of the 340-to-380 fluorescence ratio in response to 2.8 mM glucose. Cells that exhibited more than 200% of the 340-to-380 fluorescence ratio to tolbutamide were used for the analysis. Average area under the curve over the interval between 0 and 5 min (average AUC (0–5 min)) was calculated for $[Ca^{2+}]_i$ in response to 22 mM glucose, 22 mM glucose plus NERP-2, 22 mM glucose plus NERP-2-Gly, or 22 mM glucose plus GLP-1.

2.6. Statistical analysis

Statistical analyses were performed by two-way ANOVA and Bonferroni's post-test for multiple comparisons of *in vivo* experiments. In cell-culture experiments, differences among multiple groups were determined using one-way ANOVA and Fisher's LSD test. When two mean values were compared, analysis was performed by unpaired *t*-test. All data are expressed as means ± S.E.M. $P < 0.05$ was considered to be statistically significant.

3. Results

3.1. NERP-2 is co-localized with insulin

By immunostaining, NERP-1 and -2 were detected in mouse pancreatic islets (Fig. 1A and B). No signal was detected in *Vgf* knockout mouse islets (Fig. 1C and D). In double immunofluorescence histochemistry, NERP-2 was co-localized with insulin (Fig. 1E–G).

3.2. NERP-2, but neither NERP-1 nor NERP-2-Gly, potentiates GSIS

Neither NERP-1 nor NERP-2 affected insulin secretion from MIN6 cells under low glucose concentrations (5.5 mM). NERP-2 significantly potentiated GSIS (22 mM glucose), whereas NERP-1 and NERP-2-Gly had no effect on GSIS (Fig. 2A). NERP-2 also potentiated GSIS in isolated mouse islets in a dose-dependent manner, with a lowest effective dose of 10^{-7} M (Fig. 2B). This response

was also glucose-dependent, since no effect of NERP-2 was seen under low glucose. Neither NERP-1 nor NERP-2-Gly enhanced GSIS in islets (Fig. 2B).

3.3. NERP-2 enhances GSIS in vivo

Plasma insulin significantly increased 10 min after i.p. administration of NERP-2 to mice, as in the case of GLP-1 (Fig. 3A). Average AUC (0–30 min) for plasma insulin was significantly higher in response to NERP-2 than in response to glucose alone (Fig. 3B). Also when NERP-2 (1.25 μmol/kg BW) was administered to mice 30 min before glucose administration, NERP-2 significantly increased plasma insulin compared with saline plus glucose administration (average AUC (0–30 min) of NERP-2 vs saline, 9.9 ± 1.7 ng/ml·30 min vs 4.7 ± 0.5 ng/ml·30 min, $P < 0.02$). In rats as well, plasma insulin significantly increased from 1 to 30 min after i.v. administration of NERP-2 (Fig. 3C). Average AUC (0–30 min) of plasma insulin was significantly higher in response to NERP-2 than in response to glucose alone (Fig. 3D).

### 3.4. NERP-2 facilitates $[Ca^{2+}]_i$ in MIN6 cells

To determine whether NERP-2-enhanced insulin release is mediated by intracellular calcium influx ($[Ca^{2+}]_i$), we observed the 340-to-380 fluorescence ratio as a measure of $[Ca^{2+}]_i$ in MIN6 cells. We used GLP-1 as a positive control to validate the experimental conditions. In 22 mM glucose plus NERP-2, $[Ca^{2+}]_i$ increased quickly and to a significantly greater extent than in 22 mM glucose (Fig. 4, compare B vs A). The response to 22 mM glucose plus NERP-2-Gly (Fig. 4C) was similar to the response to 22 mM glucose alone. GLP-1 induced a rapid and long elevation of $[Ca^{2+}]_i$ (Fig. 4D). MIN6 cells did not respond to 2.8 mM glucose (Fig. 4E). Average AUC (0–5 min) was significantly higher after administration of NERP-2 or GLP-1 than after administration of 22 mM glucose (Fig. 4F). NERP-2-Gly did not affect $[Ca^{2+}]_i$ in MIN6 cells.

4. Discussion

Under physiologic conditions, the concentration of blood glucose fluctuates in a narrow range despite alternation between periods of food intake and fasting. Tight control of insulin secretion is regulated by glucose itself and by an array of metabolic, neural, and hormonal factors. VGF-derived NERPs were originally identified in rat hypothalamus, and were subsequently detected in hu-
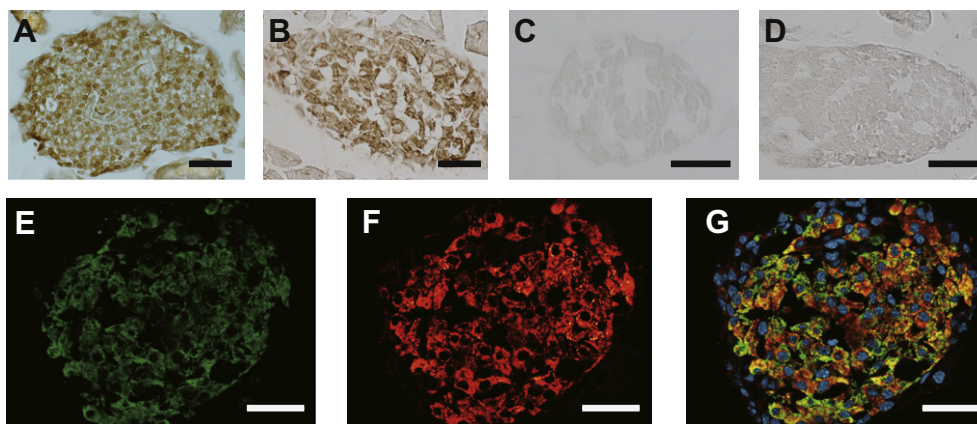
Fig. 1. Localizations of NERP-1 and NERP-2 in C57BL/6 J mouse pancreatic islets. NERP-1 (A) and NERP-2 (B) were detected as DAB-immunopositive. No immunoreactivity of NERP-1 (C) or NERP-2 (D) was detected in *Vgf* knockout mouse pancreas. Immunofluorescence staining revealed that insulin (E, green) and NERP-2 (F, red) are co-localized (G, merged) in mouse pancreatic islets. DAPI is shown in blue. Scale bars, 100 μm.
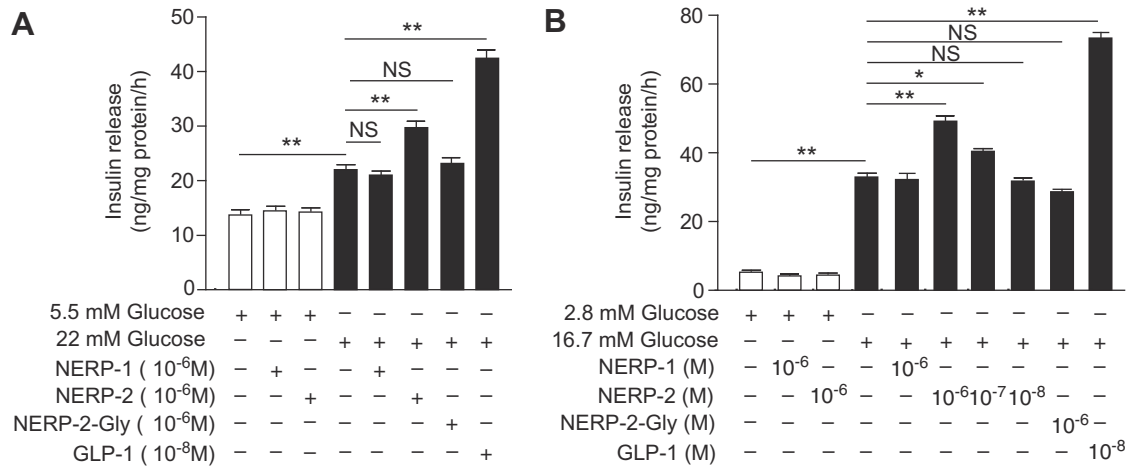
Fig. 2. Effect of NERP-2 on insulin secretion. Insulin secreted from MIN6 cells (A) or isolated mouse islets (B) was measured 1 h after administration of peptides. NERP-2 and GLP-1, but neither NERP-1 nor NERP-2-Gly, potentiated GSIS. $n = 10$ per group $^*P < 0.05$, $^{**}P < 0.01$. NS, not significant.
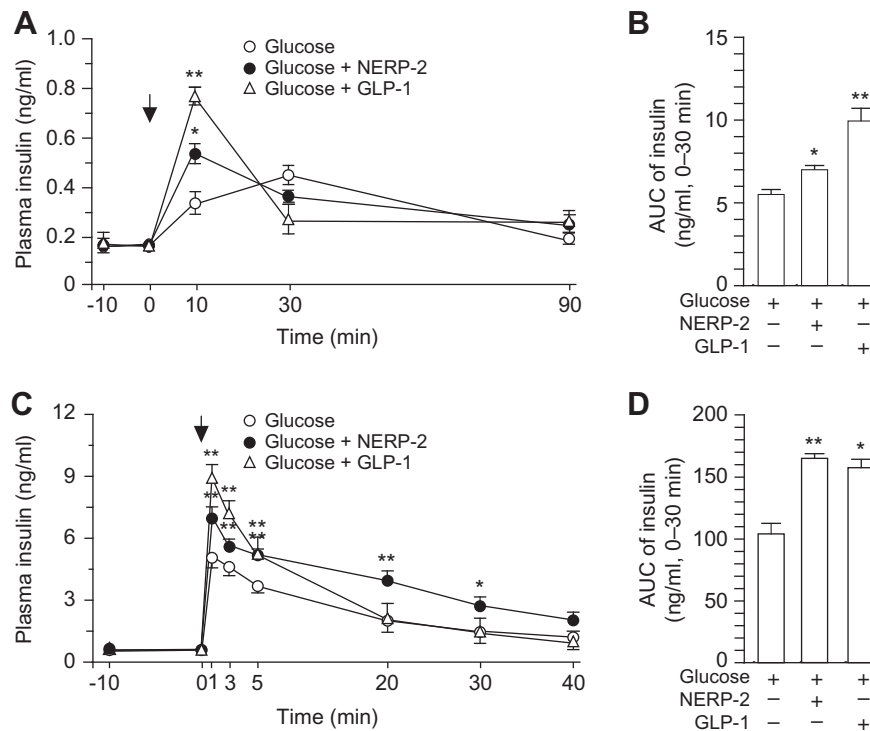

Fig. 3. NERP-2 enhances GSIS in vivo. Plasma insulin was measured after an i.p. administration of glucose to mice (A) or i.v. administration of glucose to rats (C) ($n = 6$–8 per group). Animals received glucose alone (open circles), glucose + NERP-2 (closed circles), or glucose + GLP-1 (triangles). Arrows indicated i.p. (A) or i.v. (C) injection. Average AUC (0–30 min) for plasma insulin in mice (B) and rats (D). $^*P < 0.05$, $^{**}P < 0.01$ vs glucose alone.

man pancreatic islets [10,15]. To investigate the biological activity of NERPs in the islets, we studied their expression pattern, and observed that they are co-localized with insulin in mouse islet β-cells. NERP-2, but not NERP-1, stimulated insulin secretion both in vitro and in vivo. We also found that NERP-2 potentiated GSIS in a rat pancreatic β-cells line, INS-1 cells (data not shown). C-terminal amidation of NERP-2 was essential for insulin secretion, as is the case with its activities regulating in vasopressin secretion and feeding. NERP-1 and -2 had similar potencies in suppressing vasopressin release from the hypothalamus and posterior pituitary [10], whereas only NERP-2 stimulated food intake and enhanced energy consumption via the neuropeptide orexin pathway in the hypothalamus when administered centrally to rats [11]. The in vitro experiments described here indicate that NERP-2 directly acts on β-cells to stimulate insulin secretion by increasing intracellular calcium concentration. The cell-surface receptors or target molecules of NERPs have not yet been identified; however, these findings imply that there is likely to be a receptor or a target molecule specific for NERP-2.

NERP-2 is not itself a secretagogue, and its effect on insulin secretion is evident only in the presence of hyperglycemia. This is also true for other insulinotropic peptides including GLP-1, glucose-dependent insulinotropic peptide, vasoactive intestinal polypeptide, and pituitary adenylate cyclase-activating polypeptide [16,17]. GLP-1 binds to the GLP-1 receptor expressed on β-cells, triggering an increase in cAMP and activation of Epac and PKA,
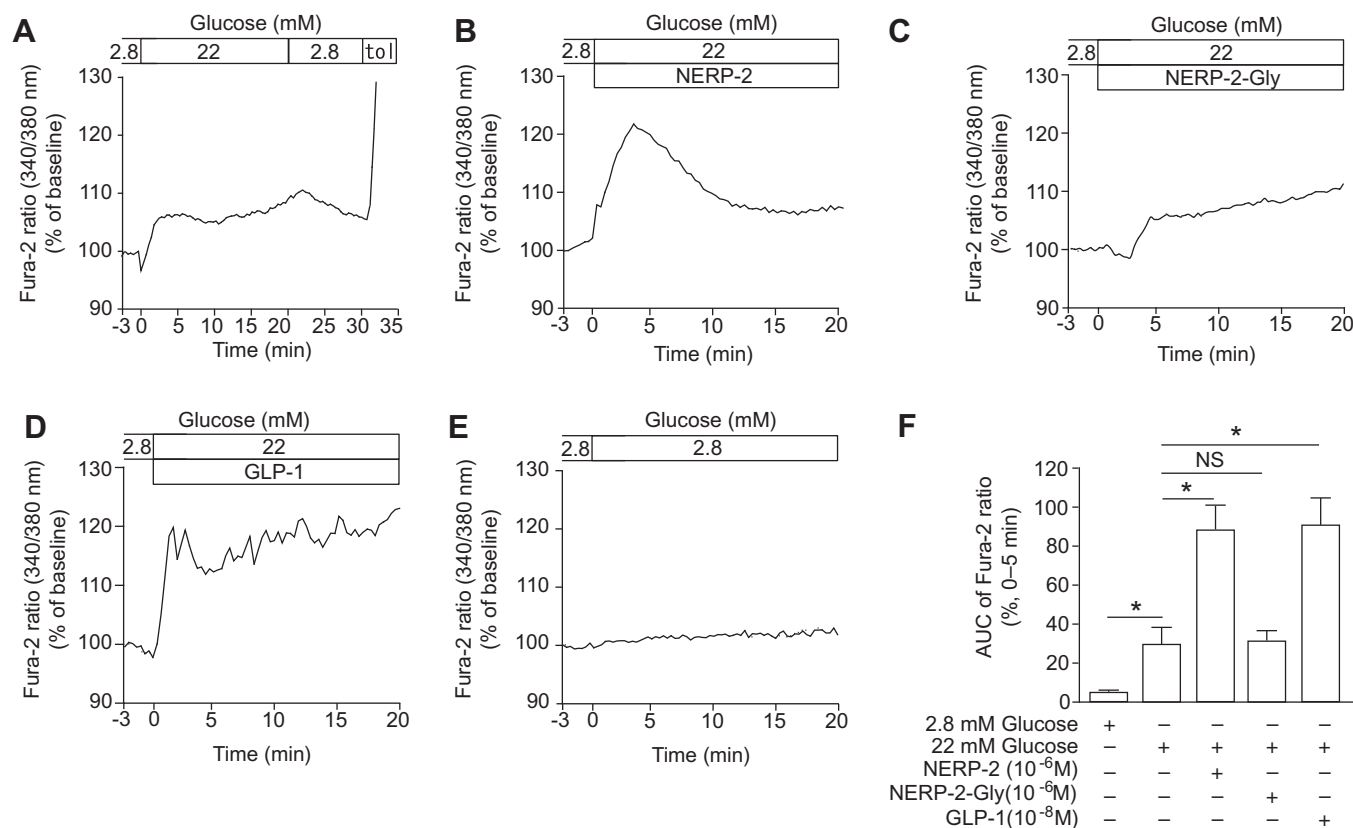
Fig. 4. NERP-2 facilitates $[Ca^{2+}]_i$ in MIN6 cells. Figures shown are representative Fura-2 ratios in response to 22 mM glucose and subsequent return to 2.8 mM glucose, followed by tolbutamide (tol) treatment (A); 22 mM glucose + 1 μM NERP-2 (B); 22 mM glucose + 1 μM NERP-2-Gly (C); 22 mM glucose + 10 nM GLP-1 (D); and 2.8 mM glucose (E) (n = 13–16 cells). MIN6 cells that responded to tolbutamide were used for the analysis of $[Ca^{2+}]_i$. (F) Average AUC (0–5 min) for $[Ca^{2+}]_i$ in (A)–(E). $*P < 0.01$. NS, not significant.

thereby causing closure of K^+_{ATP} channels, which in turn stimulates intracellular calcium influx by opening voltage-gated calcium channels. GLP-1-activated Epac and PKA also sensitize calcium channels on the endoplasmic reticulum, allowing the release of calcium from intracellular stores. These two mechanisms of increasing intracellular calcium concentration potentiate exocytosis of insulin [18,19]. The profile of NERP-2-induced calcium influx in Fig. 4 is quite different from that of GLP-1. The monophasic increase in intracellular calcium level after administration of NERP-2 suggests that this peptide stimulates intracellular calcium entry via receptor-operated channels [20,21] rather than voltage-gated calcium channels.

Very recently, another VGF-derived peptide, TLQP-21, corresponding to VGF amino acids 554–574, has been shown to potentiate GSIS is rat and human islets and improve glucose tolerance *in vivo* [22]. TLQP-21 elevates cAMP levels in rat pancreatic islets, independently of the GLP-1 pathway. *Vgf* mutant mice are sensitive to insulin and resistant to developing hyperinsulinemia on a high-calorie diet [23]. Given that NERP-2 and TLQP-21 act as insulinotropic peptides, glucose tolerance in *Vgf* knockout mice suggests that other VGF-derived peptide(s) also act as regulatory peptides that counter insulin action.

VGF-derived peptides provide autocrine, paracrine, and endocrine signals to regulate release of a variety of hormones [24]. The relatively abundant expression of NERPs in human tissues will lead to their increased utility as biomarkers of diseases and therapeutic efficacy. Collectively, the findings presented here provide a solid basis for identifying novel physiological roles of NERP-2, and the potential roles of other VGF-derived peptides, in the regulation of glucose metabolism.

References

[1] A. Levi, J.D. Eldridge, B.M. Paterson, Molecular cloning of a gene sequence regulated by nerve growth factor, Science 229 (1985) 393–395.
[2] S.R. Salton, D.J. Fischberg, K.W. Dong, Structure of the gene encoding VGF, a nervous system-specific mRNA that is rapidly and selectively induced by nerve growth factor in PC12 cells, Mol. Cell. Biol. 11 (1991) 2335–2349.
[3] S.R. Salton, Nucleotide sequence and regulatory studies of VGF, a nervous system-specific mRNA that is rapidly and relatively selectively induced by nerve growth factor, J. Neurochem. 57 (1991) 991–996.
[4] G.L. Ferri, A. Levi, R. Possenti, A novel neuroendocrine gene product: selective VGF8a gene expression and immuno-localisation of the VGF protein in endocrine and neuronal populations, Mol. Brain Res. 13 (1992) 139–143.
[5] S.R. Salton, G.L. Ferri, S. Hahm, et al., VGF: a novel role for this neuronal and neuroendocrine polypeptide in the regulation of energy balance, Front. Neuroendocrinol. 21 (2000) 199–219.
[6] A. Bartolomucci, G.L. Corte, R. Possenti, et al., TLQP-21, a VGF-derived peptide, increases energy expenditure and prevents the early phase of diet-induced obesity, Proc. Natl. Acad. Sci. USA 103 (2006) 14584–14589.
[7] P.H. Jethwa, A. Warner, K.N. Nilaweera, et al., VGF-derived peptide, TLQP-21, regulates food intake and body weight in siberian hamsters, Endocrinology 148 (2007) 4044–4055.
[8] J. Alder, S.T. Varia, D.A. Bangasser, et al., Brain-derived neurotrophic factor-induced gene expression reveals novel actions of VGF in hippocampal synaptic plasticity, J. Neurosci. 23 (2003) 10800–10808.
[9] J.G. Hunsberger, S.S. Newton, A.H. Bennett, et al., Antidepressant actions of the exerciseregulated gene VGF, Nat. Med. 13 (2007) 1476–1482.

[10] H. Yamaguchi, K. Sasaki, Y. satomi, et al., Peptidomic identification and biological validation of neuroendocrine regulatory peptide-1 and -2, J. Biol. Chem. 282 (2007) 26354–26360.

[11] K. Toshinai, H. Yamaguchi, H. Kageyama, et al., Neuroendocrine regulatory peptide-2 regulates feeding behavior via the orexin system in the hypothalamus, Am. J. Physiol. Endocrinol. Metab. 299 (2010) E394–E401.

[12] S. Hahm, T.M. Mizuno, T.J. Wu, et al., Targeted deletion of the Vgf gene indicates that the encoded secretory peptide precursor plays a novel role in the regulation of energy balance, Neuron 23 (1999) 537–548.

[13] A. Lernmark, Isolated mouse islets as a model for studying insulin release, Acta Diabetol. Lat. 8 (1971) 649–679.

[14] K. Toshinai, H. Yamaguchi, Y. Sun, et al., Des-acyl ghrelin induces food intake by a mechanism independent of the growth hormone secretagogue receptor, Endocrinology 147 (2006) 2306–2314.

[15] T. Matsuo, H. Yamaguchi, H. Kageyama, et al., Localization of neuroendocrine regulatory peptide-1 and -2 in human tissues, Regul. Pept. 163 (2010) 43–48.

[16] M.S. Winzell, B. Ahren, Role of VIP and PACAP in islet function, Peptides 28 (2007) 1805–1813.

[17] W. Kim, J.M. Egan, The role of incretins in glucose homeostasis and diabetes treatment, Pharmacol. Rev. 60 (2008) 470–512.

[18] A.R. Meloni, M.B. DeYoung, C. Lowe, et al., GLP-1 receptor activated insulin secretion from pancreatic β-cells: mechanism and glucose dependence, Diabetes Obes. Metab. in press.

[19] S. Seino, Cell signalling in insulin secretion: the molecular targets of ATP, cAMP and sulfonylurea, Diabetologia 55 (2012) 2096–2108.

[20] C. Fasolato, P. Pizzo, T. Pozzan, Receptor-mediated calcium influx in PC12 cells. ATP and bradykinin activate two independent pathways, J. Biol. Chem. 265 (1990) 20351–20355.

[21] C.C. Felder, M.O. Poulter, J. Wess, Muscarinic receptor-operated Ca^{2+} influx in transfected fibroblast cells is independent of inositol phosphates and release of intracellular Ca^{2+}, Proc. Natl. Acad. Sci. USA 89 (1992) 509–513.

[22] S.B. Stephens, J.C. Schisler, H.E. Hohmeier, et al., A VGF-derived peptide attenuates development of type 2 diabetes via enhancement of islet β-cell survival and function, Cell Metab. 16 (2012) 33–43.

[23] E. Watson, S. Hahm, T.M. Mizuno, et al., VGF ablation blocks the development of hyperinsulinemia and hyperglycemia in several mouse models of obesity, Endocrinology 146 (2005) 5151–5163.

[24] A. Bartolomucci, R. Possenti, S.K. Mahata, et al., The extended granin family: structure, function, and biomedical implications, Endocr. Rev. 32 (2011) 755–797.